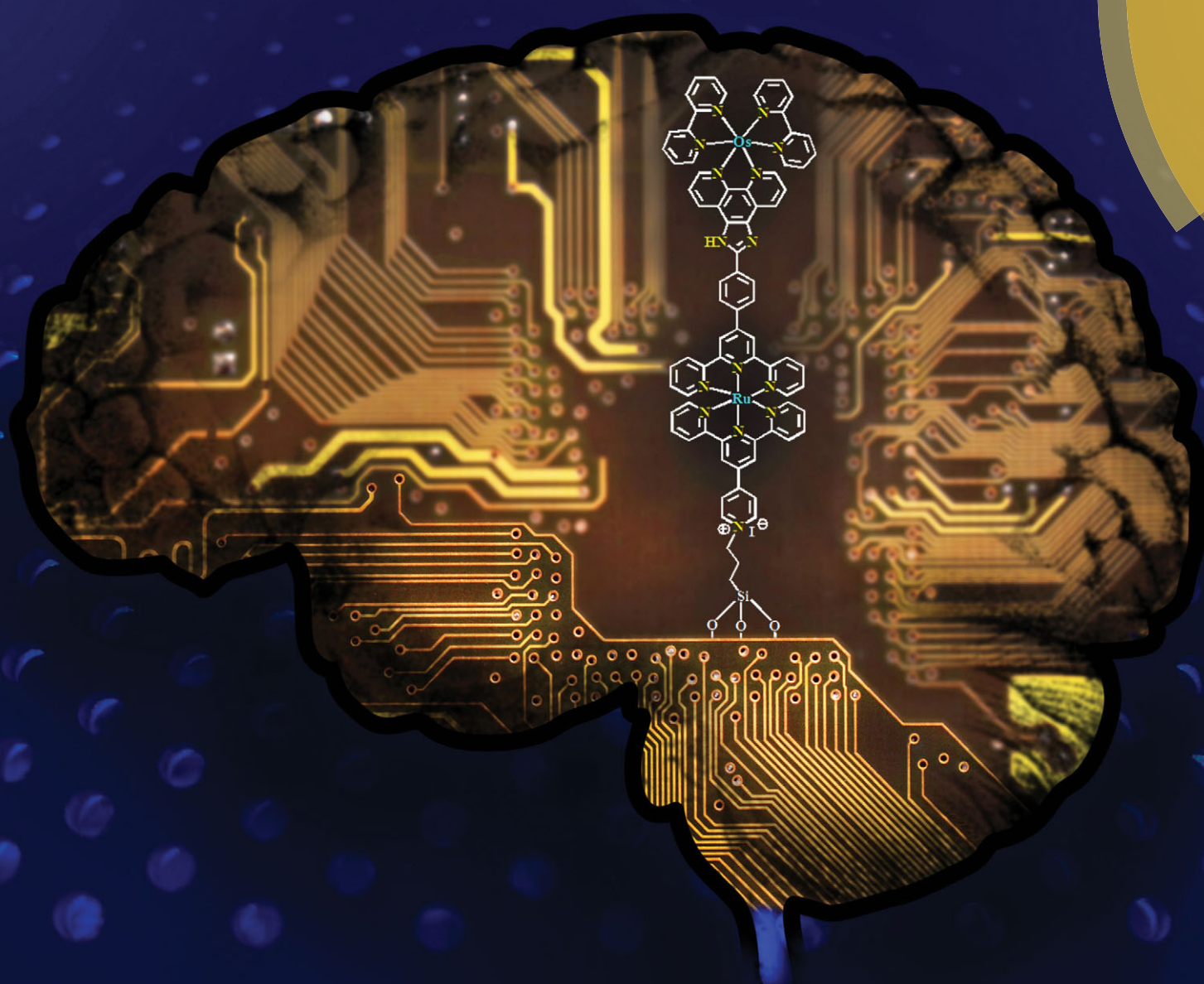


# ChemComm

Chemical Communications

www.rsc.org/chemcomm



ISSN 1359-7345



**COMMUNICATION**

Rinkoo D. Gupta, Antonino Gulino *et al.*

A ternary memory module using low-voltage control over optical properties of metal-polypyridyl monolayers

# A ternary memory module using low-voltage control over optical properties of metal-polypyridyl monolayers†‡

Cite this: *Chem. Commun.*, 2014, 50, 3783

Received 16th January 2014,  
Accepted 7th February 2014

DOI: 10.1039/c4cc00388h

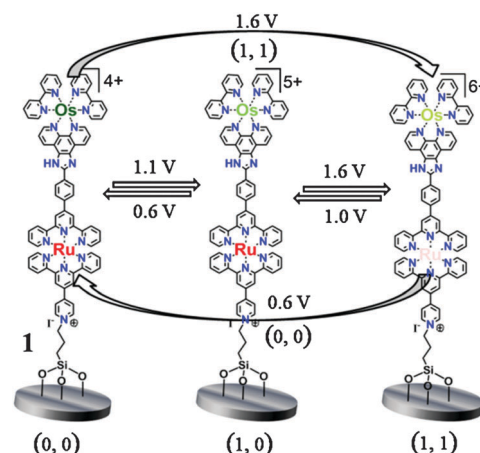
www.rsc.org/chemcomm

Anup Kumar,<sup>a</sup> Megha Chhatwal,<sup>a</sup> Prakash Chandra Mondal,<sup>a</sup> Vikram Singh,<sup>a</sup> Alok Kumar Singh,<sup>a</sup> Domenico A. Cristaldi,<sup>b</sup> Rinkoo D. Gupta\*<sup>c</sup> and Antonino Gulino\*<sup>b</sup>

A ternary memory module has been designed as a function of precise voltage command. The monolayer based module displays perpetual stability and non-hysteretic reversibility for multiple scans ( $10^2$ ). Ternary-state readout provides a vision to integrate the next generation of “smart electro-optical devices” viable for multi-state memory.

Smart surfaces<sup>1</sup> find potential impetus for advanced memory storage/processing<sup>2</sup> via commutable redox-states. In this context, distinct redox-states are highly recommended for realization of multi-memory enabled molecular devices.<sup>3</sup> Notably, the control over multi-redox states<sup>4</sup> potentially ensures rapid information storage/transfer for molecular-memory. In this aspect, spectro-electrochemical control over a hetero-redox-centred monolayer is highly imperative and rarely exploited thus far.<sup>5</sup> Herein, we assessed the electro-optical tuning of the especially designed hetero-bimetallic complex based monolayer (**1**) comprising two redox-active data saving bits ( $\text{Ru}^{2+}$  and  $\text{Os}^{2+}$ ) and a conductive imidazole aromatic spine (Scheme 1).

The siloxane-based monolayers of **1** were fabricated on the Si(100)/ITO-coated glass substrate by adopting a previously reported method.<sup>6</sup> The integrity of molecules on the surface was verified with a combination of surface analysis techniques such as X-ray photo-electron spectroscopy (XPS), semicontact atomic force microscopy (AFM), and optical transmission and electrochemistry. The surface morphology investigated by AFM revealed a homogeneous monolayer (Fig. S1, left, ESI†). The root mean square roughness of the monolayer was typically around 0.9 nm with a height distribution centred at 2.8 nm (Fig. S1, right, ESI†). The molecular characterization of the **1**-Si(100) monolayer was carried out by XPS.<sup>7</sup>



Scheme 1 Representation of electro-optical tuning of the **1**-ITO monolayer under precise potential command.

As a general observation, the atomic concentration analyses, performed at all the investigated photoelectron take-off angles, have shown that the substrate signals increase and the monolayer signals decrease on going from low ( $5^\circ$ ) to high ( $80^\circ$ ) angles. Moreover, atomic concentration analyses always indicated the Os 4f, Ru 3p and N 1s signals in the 1 : 1 : 15 intensity ratios, once corrected for the relevant atomic sensitivity factors. Spectral fitting of the N 1s signal reveals the presence of two components in the 1 : 15 ratio (Fig. 1). These two peaks lie at 399.8 and 402.3 eV. As a consequence, the component at 399.8 is assigned as a whole to all polypyridyl nitrogens of **1**. The higher energy component is consistent with the quaternized nitrogen of a pyridine moiety.<sup>8</sup> Fig. S2 (ESI†) shows the Os 4f spin-orbit components at 51.0 and 53.8 eV, consistent with the Os(II) oxidation state. In analogy, Ru 3p levels lying at 462.4 and 486.6 eV are consistent with the presence of the Ru(II) state (Fig. S3, ESI†).<sup>9</sup>

The cyclic voltammogram of the **1**-ITO monolayer showed two reversible redox waves at  $E_{1/2} = 0.97$  and 1.38 V attributed to  $\text{Os}^{2+/3+}$  and  $\text{Ru}^{2+/3+}$  redox couples respectively (Fig. 2a).<sup>10</sup> The redox waves

<sup>a</sup> Department of Chemistry, University of Delhi, New Delhi-110 007, India

<sup>b</sup> Dipartimento di Scienze Chimiche, Università di Catania, and INSTM Udr of Catania, viale A. Doria 6, 95125 Catania, Italy. E-mail: agulino@unict.it

<sup>c</sup> Faculty of Life Sciences and Biotechnology, South Asian University, New Delhi-110 021, India. E-mail: rdgupta@sau.ac.in

† A tribute to Late Dr Tarkeshwar Gupta.

‡ Electronic supplementary information (ESI) available: Experimental details, characterization, and electrochromic results in solution. See DOI: 10.1039/c4cc00388h

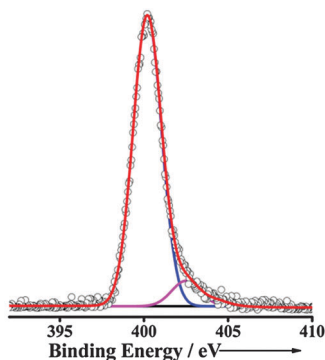


Fig. 1 Monochromatized Al-K $\alpha$  excited XPS at a photoelectron take-off angle of 45° for the **1-Si(100)** monolayer in the N 1s binding energy region. The experimental spectral data points (open circles) are fitted with two dominant Gaussians at 399.8 (red line) and 402.3 (magenta line) eV.

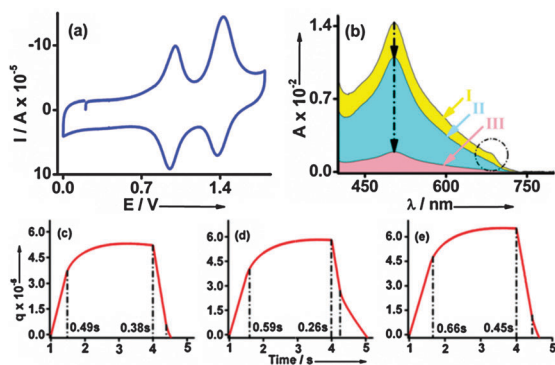


Fig. 2 Cyclic voltammogram of the as-synthesized **1-ITO** monolayer at 1.0 V s<sup>-1</sup> (vs. Ag/AgCl, 20 mM Bu<sub>4</sub>NClO<sub>4</sub>-CH<sub>3</sub>CN). (a) Spectro-electrochemical switching of the **1-ITO** monolayer (3.0 × 0.8 cm) using triple-step potentials of 0.6, 1.1, and 1.6 V. (b) Chrono-coulometry experiment at 0.6–1.1 V (c) and 0.6–1.6 V (d) and 0.6–1.6 V (e) for 3 s.

followed the characteristics of typical surface-confined molecules. The peak current densities ( $I_{pa}$  and  $I_{pc}$ ) increase linearly with the scan rate (Fig. S4, ESI†).<sup>11</sup> Furthermore, the peak separation ( $\Delta E$ ) of order < 20 mV was observed at lower scan rates followed by a gradual enhancement at higher scan rates due to  $iR$ -drop and/or the influence of heterogeneous electron-transfer kinetics on the surface.<sup>12</sup> The operational stability of the **1-ITO** monolayer under the potential domain (0.0–1.8 V) was judged by running the continuous read–write cycles ( $10^2$ ) (Fig. S5, ESI†). Consequently, the cyclic voltammogram displayed a slight variation (*ca.* 8%) for initial conditioning scans, which could be assigned to deactivation/reordering of molecular components.<sup>6</sup> Additionally, UV-vis and mass spectra of the electrolytic solution after  $10^2$  cycles revealed the absence of any complex and imply the desired robustness of the system against the imposed voltage domain. The UV-vis spectrum of the **1-ITO** monolayer showed characteristic singlet and triplet metal-to-ligand charge transfer bands (<sup>1</sup>MLCT and <sup>3</sup>MLCT) centred at  $\lambda_{max} = 503$  and 687 nm respectively. These two bands revealed a bathochromic shift ( $\Delta\lambda$ ) of 8 and 40 nm, respectively, w.r.t. solution measurements due to the formation of a pyridinium salt.<sup>13</sup> The footprint (from UV-vis)/surface

coverage (from CV), estimated as  $\sim 90$ – $110$  Å<sup>2</sup> per molecule, indicated a compact film, which is in agreement with previous reports.<sup>14</sup> Interestingly, the optical identity of **1** *i.e.*, singlet and triplet MLCT bands were tuned to exhibit three distinct absorbance states upon varying the electrical input and thereby supporting the viability of **1** as a multiple charge/information storage module. For instance, the <sup>1</sup>MLCT band ( $\lambda_{max} = 503$  nm) revealed a hypochromic shift (on/off ratio, 1.4 : 1 on ITO, 1.7 : 1 in solution) along with the vanishing of <sup>3</sup>MLCT ( $\lambda_{max} = 687$  nm) upon applying a voltage range of 0.6–1.1 V (Fig. 2b). This spectral perturbation can be assigned to the exclusive oxidation of Os<sup>2+</sup> in **1**.<sup>1b</sup> However, the observed low on/off ratio could be due to the substantial contribution of Ru<sup>2+</sup> in <sup>1</sup>MLCT and the considerable distance of Os<sup>2+</sup> from the ITO surface ( $\sim 30$  Å estimated using the Chem3D Pro energy minimization model).<sup>4a</sup> Furthermore, upon imposing the potential range of 1.0–1.6 V, the absorbance of the <sup>1</sup>MLCT further reduced (on-off ratio 5 : 1), which is attributed to the oxidation of both (Ru<sup>2+</sup> and Os<sup>2+</sup>) redox-species in **1**.<sup>4</sup> Notably, rapid response time was observed for this charge based bit-storage/release (*i.e.*, 0.49 s/0.38 s for Os<sup>2+/3+</sup>, 0.59 s/0.26 s for Os<sup>3+</sup> and Ru<sup>2+/3+</sup>) as depicted in Fig. 2c and d respectively. Noticeably, the **1-ITO** monolayer can produce three-state absorbance changes *i.e.*, I (absorbance threshold = 0.014, Os<sup>2+</sup> and Ru<sup>2+</sup>), II (absorbance threshold = 0.010, Os<sup>3+</sup> and Ru<sup>2+</sup>) and III (absorbance threshold = 0.002, Os<sup>3+</sup> and Ru<sup>3+</sup>) under the applied potential of 0.6, 1.1 and 1.6 V respectively. Moreover, overall optical changes could be produced in a single-step by applying a wider potential range (0.6–1.6 V) in  $\sim 0.7$  s (Fig. 2e). The spectral deviation was estimated to be  $\sim 6$ – $10\%$  for three experiments using the same set-up (Fig. S6, ESI†). The transduction of the voltage input into precise optical readout has been demonstrated in solution also (Fig. S7–S9, ESI†).

Note that, the presence of three distinct optical states I, II, and III could be exploited for integration of interchangeable binary and ternary memory states as a function of applied voltage.<sup>2b,15</sup> To mimic the memory elements, oxidation and reduction under each redox wave can be considered as writing “1” and erasing “0” of data by assuming the principle of binary logic.<sup>16</sup> Thus, binary memory states could be constructed by applying a broad potential range (0.6–1.6 V), capable of writing/erasing the data at the double redox moieties under single command for processing of multibits (“00”–“11”) of the same information. However, successive knocking at redox moieties *viz.* “00”, “10” and “11” might construct a commutable ternary memory state under variable voltages.<sup>2a</sup>

Both reversibility and stability are important parameters for a device-quality monolayer. Thus, the **1-ITO** monolayer was amperometrically subjected to switching potentials (0.6, 1.1 and 1.6 V, 3 s) for repetitive cycles and the corresponding absorbance change at  $\lambda_{max} = 503$  nm was monitored as a function of time (Fig. 3). A minimal signal loss (*ca.* 10%) was observed after attaining 100 cycles for all states *i.e.*, I, II, and III using the same monolayer, probably due to minor leaching of molecules from the surface under the potential stress. However, significant signal loss ( $\Delta A = \sim 45\%$ ) was observed upon scanning at potentials > 2.0 V and < 0.0 V. The redox states *i.e.*,

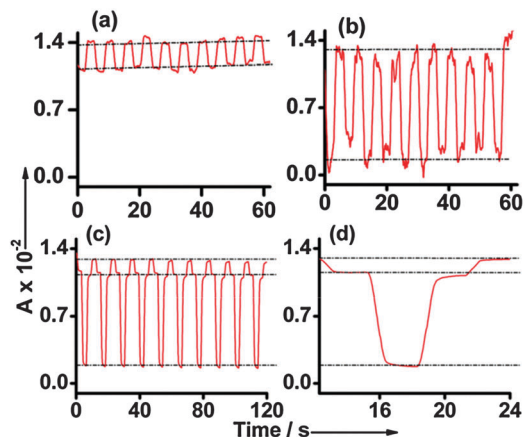


Fig. 3 Chrono-absorptometry switching experiment at  $\lambda = 503$  nm for  $\text{Os}^{2+}$  (a, 0.6–1.1 V),  $\text{Ru}^{2+}$  and  $\text{Os}^{2+}$  (b, 0.6–1.6 V), successive knocking at each metal centre (c, 0.6–1.1–1.6–1.0 V) with a magnified view of a single cycle (d), for 3 min in 20 mM TBAP in acetonitrile.

**II** and **III** were stable under the nitrogen atmosphere for 5 min, whereas regained state **I** under air within 50 and 70 s, respectively, due to reduction by adventitious moisture under the open circuit conditions.<sup>17</sup> In addition, XPS after attaining 100 cycles revealed atomic concentration values close to those of the starting monolayer (within the experimental errors  $\pm 5\%$ ).

Furthermore, most of the electronic devices suffer from the loss of functioning because of the mechanical heat released during prolonged-work schedules. Thus, stability and functioning at elevated temperature was judged by heating the module at 200 °C for 50 h and also by stepping-up the temperature from 25 to 250 °C in a programmable fashion with a time interval of 1 h. No significant UV-vis signal and switching magnitude loss was observed for the monolayer after the heat treatment (Fig. S11, ESI†). Hence, the module successfully displays the tendency to store and hold the data under/after mechanical heat.

In summary, the **1-ITO** monolayer was exploited for ternary/binary data storage with non-destructive optical identity owing to its excellent stability and reversibility. The robustness of the system enabled it to overcome both potential stress and mechanical heat. The commutable binary and/or ternary state has demonstrated accurate control of voltage over optical threshold and can offer potential alternative to real devices such as DRAM, SRAM and FLASH memory. Indeed, intact functioning under long term potential stress and at elevated temperature is attractive for future electronics.

The authors gratefully thank the Department of Science and Technology (SERB/F/1448/2012-13), New Delhi and the

University of Delhi, Delhi, for financial support. A.K. thanks UGC for providing Senior Research Fellowship. A. Gulino thanks the Ministero dell'Università e della Ricerca (MIUR) for the RINAME (grant number RBAP114AMK) and also the University of Catania.

## Notes and references

- (a) C. Simão, M. Mas-Torrent, N. Crivillers, V. Lloveras, J. M. Artés, P. Gorostiza, J. Veciana and C. Rovira, *Nat. Chem.*, 2011, **3**, 359–364; (b) L. Motiei, M. Lahav, D. Freeman and M. E. van der Boom, *J. Am. Chem. Soc.*, 2009, **131**, 3468–3469.
- (a) T. Gupta, P. C. Mondal, A. Kumar, Y. L. Jeyachandran and M. Zharnikov, *Adv. Funct. Mater.*, 2013, **23**, 4227–4235; (b) G. de Ruiter and M. E. van der Boom, *Acc. Chem. Res.*, 2011, **44**, 563–573.
- (a) C. Simão, M. Mas-Torrent, J. C. Montenegro, F. Otón, J. Veciana and C. Rovira, *J. Am. Chem. Soc.*, 2011, **133**, 13256–13259; (b) D. Margulies, G. Melman and A. Shanzer, *Nat. Mater.*, 2005, **4**, 768–771.
- (a) G. de Ruiter, M. Lahav, G. Evmenenko, P. Dutta, D. A. Cristaldi, A. Gulino and M. E. van der Boom, *J. Am. Chem. Soc.*, 2013, **135**, 16533–16544; (b) C. J. Yao, Y. W. Zhong, H. J. Nie, H. D. Abruna and J. Yao, *J. Am. Chem. Soc.*, 2011, **133**, 20720–20723.
- G. De Ruiter, L. Motiei, J. Choudhury, N. Oded and M. E. van der Boom, *Angew. Chem., Int. Ed.*, 2010, **49**, 4780–4783.
- A. D. Shukla, A. Das and M. E. van der Boom, *Angew. Chem., Int. Ed.*, 2005, **44**, 3237–3240.
- (a) A. Gulino, *Anal. Bioanal. Chem.*, 2013, **405**, 1479–1495; (b) A. Gulino, R. G. Egdell and I. Fragalà, *J. Mater. Chem.*, 1996, **11**, 1805–1809.
- (a) R. Kaminker, L. Motiei, A. Gulino, I. Fragalà, L. J. W. Shimom, G. Evmenenko, P. Dutta, M. A. Iron and M. E. van der Boom, *J. Am. Chem. Soc.*, 2010, **132**, 14554–14561; (b) J. Choudhury, R. Kaminker, L. Motiei, G. de Ruiter, M. Morozov, F. Lupo, A. Gulino and M. E. van der Boom, *J. Am. Chem. Soc.*, 2010, **132**, 9295–9297.
- (a) A. Gulino, T. Gupta, M. Altman, S. Lo Schiavo, P. G. Mineo, I. L. Fragalà, G. Evmenenko, P. Dutta and M. E. van der Boom, *Chem. Commun.*, 2008, 2900–2902; (b) A. Gulino, T. Gupta, P. G. Mineo and M. E. van der Boom, *Chem. Commun.*, 2007, 4878–4880.
- E. Figgemeier, E. C. Constable, C. E. Housecroft and Y. C. Zimmermann, *Langmuir*, 2004, **20**, 9242–9248.
- T. Gupta, R. Cohen, G. Evmenenko, P. Dutta and M. E. van der Boom, *J. Phys. Chem. C*, 2007, **111**, 4655–4660.
- (a) D. A. Walsh, T. E. Keyes and R. J. Forster, *J. Phys. Chem. B*, 2004, **108**, 2631–2636; (b) A. J. Bard and L. R. Faulkner, *Electrochemical Methods: Fundamentals and Applications*, 2nd ed, John Wiley & Sons, New York, 2001.
- A. D. Shukla, D. Strawser, A. C. B. Lucassen, D. Freeman, H. Cohen, D. A. Jose, A. Das, G. Evmenenko, P. Dutta and M. E. Van der Boom, *J. Phys. Chem. B*, 2004, **108**, 17505–17511.
- (a) M. M. Walczak, D. D. Popenoe, R. S. Deinhammer, B. D. Lamp, C. Chung and M. D. Porter, *Langmuir*, 1991, **7**, 2687–2693; (b) T. Gupta and A. Kumar, *Analyst*, 2011, **136**, 4127–4129.
- (a) S. L. Hurst, *IEEE Trans. Comput.*, 1984, **c-33**, 1160–1179; (b) D. E. Knuth, *The Art of Computer Programming: Numerical Algorithms*, 3rd ed., Addison-Wesley, Reading, MA, 1997.
- T. Gupta and M. E. van der Boom, *Angew. Chem., Int. Ed.*, 2008, **47**, 5322–5326.
- T. Gupta and M. E. van der Boom, *J. Am. Chem. Soc.*, 2006, **128**, 8400–8401.